

Nanoscale

Accepted Manuscript



This is an *Accepted Manuscript*, which has been through the Royal Society of Chemistry peer review process and has been accepted for publication.

Accepted Manuscripts are published online shortly after acceptance, before technical editing, formatting and proof reading. Using this free service, authors can make their results available to the community, in citable form, before we publish the edited article. We will replace this *Accepted Manuscript* with the edited and formatted *Advance Article* as soon as it is available.

You can find more information about *Accepted Manuscripts* in the [Information for Authors](#).

Please note that technical editing may introduce minor changes to the text and/or graphics, which may alter content. The journal's standard [Terms & Conditions](#) and the [Ethical guidelines](#) still apply. In no event shall the Royal Society of Chemistry be held responsible for any errors or omissions in this *Accepted Manuscript* or any consequences arising from the use of any information it contains.

ARTICLE

Gold Nanoparticles-Packed Microdisks for Multiplex Raman Labelling of Cells

Cite this: DOI: 10.1039/x0xx00000x

Peipei Zhang^a, Junfei Xia^a, Zhibin Wang^a, Jingjiao Guan^{a,b,*}Received 00th January 2012,
Accepted 00th January 2012

DOI: 10.1039/x0xx00000x

www.rsc.org/

Micro/nanoparticles containing densely packed gold nanoparticles (AuNPs) possess unique properties potentially useful for various biomedical applications. The micro/nanoparticles are conventionally produced by the bottom-up methods, which have limited capability for controlling particle size, shape and structure. This article reports development of a top-down method that integrates layer-by-layer assembly and microcontact printing to fabricate disk-shaped microparticles named microdisks composed of densely packed AuNPs. The method allows for precise control of not only size, shape and structure of the microdisks but also amount of the AuNPs in the microdisks. The microdisks can be loaded with different Raman reporters to generate characteristic surface-enhanced Raman scattering spectra under the near infrared excitation over a centimetre-scale lens-sample distance. Moreover, the microdisks can be attached to single live cells. This microdisk platform holds potential for multiplex Raman labelling of therapeutic cells for in vivo tracking of the cells.

Introduction

Gold nanoparticles (AuNPs) promise to be useful for a variety of biomedical applications.¹ While the AuNPs are most often used in the form of individual particles, recent years have seen growing interests in assembling many AuNPs into a micro/nanoparticle with new functionalities unattainable by the individuals. In one method, AuNPs were coated on SiO₂ or CaCO₃ microparticles and the functionalized microparticles were used as colloidal probes for Raman detection of biomolecules.^{2,3} In a second method, hollow microcapsules were produced by coating template microparticles with AuNPs and polyelectrolytes through layer-by-layer (LbL) assembly followed by dissolving the microparticles.^{4,5,6} The aggregated AuNPs in the microcapsules allowed enhanced Raman imaging and photo-triggered release of cargos in the microcapsules via photothermal conversion. In a third method, AuNPs were self-assembled into hollow vesicles of 200-300 nm in diameter.^{7,8,9,10} The densely packed AuNPs were able to promote light absorption in the near infrared (NIR) range, Rayleigh and Raman scattering, photoacoustic imaging or photothermal conversion.

These capabilities render the AuNPs-packed micro/nanoparticles highly attractive for various biomedical applications.

A common feature shared by the above methods for producing the AuNPs-packed micro/nanoparticles is the use of the bottom-up approach, which typically suffers from limited ability to control particle size, shape and structure as exemplified by the roughly spherical shape of the above-mentioned particles. In contrast, top-down methods are able to fabricate particles with precisely controlled sizes, non-spherical shapes and well-defined internal structures that are desirable or even essential for various biomedical applications.^{11,12,13,14,15} Notably, Rubner *et al.* combined LbL assembly and photolithography to produce multilayered,

polyelectrolyte-based, and plate-shaped microparticles containing magnetic nanoparticles.¹⁶ We also developed a simple, inexpensive and highly versatile method for fabricating multilayered polyelectrolyte microparticles by integrating LbL assembly and microcontact printing.¹⁷ In this study, we extend this method to the fabrication of microparticles containing densely packed AuNPs. The microparticles are disk-shaped and thus termed microdisks hereafter.

Our microdisks are intended to be used for tracking cells based on Raman imaging. The ability to track therapeutic cells *in vivo* is useful for developing effective cell therapies. Existing cell-tracking techniques including magnetic resonance imaging, positron emission tomography and quantum dot-based NIR fluorescence imaging suffer from the need for ionizing radiation, use of toxic quantum dots, or limited capability for multiplexing labelling.^{18,19,20} In contrast, the AuNPs are less toxic than the quantum dots.¹ Raman imaging does not involve ionizing radiation. Moreover, Raman imaging allows superb multiplexing capability because Raman spectra have narrow bandwidths and are highly material dependent. It should also be noted that Raman spectra can be excited by NIR, which permits a tissue-penetration depth at the centimetre scale.²¹ In addition, the unique shape of the microdisk can promote its adhesion to cells.¹⁴ We thus believe that our microdisk platform is suitable for tracking cells based on Raman imaging. This study focuses on demonstrating the feasibility of multiplex Raman labelling of cells with the microdisks.

Experimental section

Our fabrication method is illustrated in Figure 1. Briefly, a polyelectrolyte multilayer was first formed on an unmodified poly(dimethyl siloxane) (PDMS) stamp bearing an array of

micropillars.²² Negatively charged AuNPs and positively charged poly(diallyldimethyl ammonium chloride) (PDAC) were then deposited on the stamp sequentially as a bilayer. This step could be

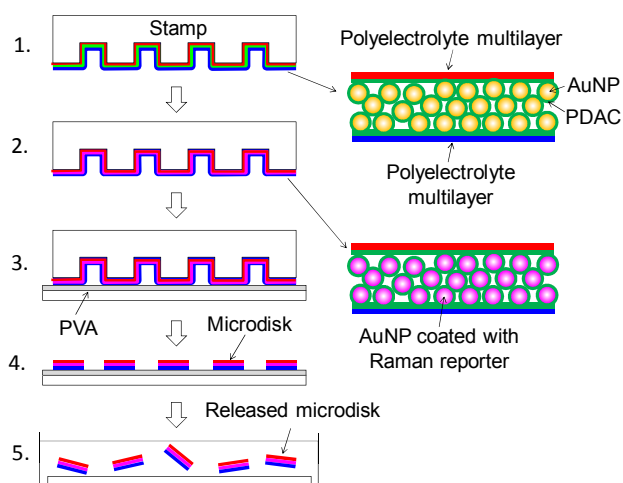


Figure 1. Procedure for fabricating AuNPs-packed microdisks loaded with a Raman reporter. Steps: (1) Deposit a multilayer of AuNPs and polyelectrolytes including poly(diallyldimethyl ammonium chloride) (PDAC) on a stamp; (2) Load the Raman reporter molecules into the microdisks; (3) Place the stamp on a glass slide coated with a thin film of poly(vinyl alcohol) (PVA); (4) Remove the stamp to leave the microdisks on the PVA film; and (5) Release the microdisks by dissolving PVA.

repeated to build multiple AuNPs/PDAC bilayers. 10 nm-diameter AuNPs were used throughout this study unless otherwise noted. Next, the stamp was coated with a second polyelectrolyte multilayer. The composition of the entire composite multilayer is expressed with notation $A/(B/C)_n$, where A, B and C refer to specific layer materials with A representing the first layer applied on to the stamp and n the number of B/C bilayers. In addition to PDAC, two other polyelectrolytes, poly(sodium 4-styrene sulfonate) (PSS) and polyallylamine hydrochloride (PAH), were used in this study. Raman reporter was loaded into the multilayer by soaking the stamp in an ethanol solution of the reporter. This step was performed only when producing microdisks for Raman spectroscopy characterization. The microdisks were generated by transferring the multilayer on the top of the micropillars to a glass slide coated with a thin film of poly(vinyl alcohol) (PVA) via physical contact. The microdisks could be released from the slide by dissolving the PVA film with water.

Materials. Poly(sodium 4-styrene sulfonate) [PSS, molecular weight (Mw): 70,000 g/mol], poly(diallyldimethyl ammonium chloride) (PDAC, Mw: 100,000-200,000 g·mol⁻¹), polyallylamine hydrochloride (PAH, Mw: 15,000 g·mol⁻¹), acid terminated poly(D, L-lactide-co-glycolide) (PLGA, lactide : glycolide = 75 : 25, Mw: 4,000-15,000 g·mol⁻¹) and 2-mercaptoethanol (BME) were purchased from Sigma-Aldrich. Glass slides, rhodamine isothiocyanate (RITC), 2-naphthalenethiol, 4-aminothiophenol and thiolphenol were purchased from VWR. Poly(vinyl alcohol) (PVA, Mw: 3000 g·mol⁻¹, 88% hydrolyzation) were purchased from Scientific Polymer Products Inc (Ontario, NY, USA). Sylgard 184 poly(dimethyl siloxane) (PDMS) kit was purchased from Dow Corning. Suspension of AuNPs with diameter of 10 nm was purchased from Ted Pella (Redding, CA, USA). Zeta potential of the AuNPs was measured as -22 mV. K562 cells were purchased from the American Type Culture Collection.

Fluorescence labelling of PAH. PAH was mixed with RITC in water at a 5,000:1 molar ratio (repeat units of PAH to RITC molecules) and kept for 24 h at room temperature. The solution was dialyzed against deionized water using a membrane with molecular weight cut-off of 20,000 g·mol⁻¹ for 24 h to remove the unreacted RITC.

Cell culture. K562 cells were cultured in RPMI 1640 medium supplemented with 10 vol% cosmic calf serum, 100 units·mL⁻¹ of penicillin and 100 µg·mL⁻¹ streptomycin at 37 °C and 5% CO₂.

Preparation of stamps. A silicon wafer master carrying a pattern of photoresist was prepared by standard photolithography. Prepolymer and curing agent of the kit was mixed at a 10:1 weight ratio and casted on the master at 37 °C for 24 h. The stamp contained an array of circular pillars (diameter: 8 µm, height: 3.4 µm) in the square lattice with a centre-to-centre distance of 20 µm.

Preparation of PVA-coated glass slides and silicon wafers. Aqueous PVA solution (800 µL, 5 wt%) was spin-coated on a glass slide or a silicon wafer at 2,500 revolutions per min (RPM) for 3 min.

Synthesis of gold nanoparticles (AuNPs). The method developed by Jana *et al.* was used here to prepare suspensions of AuNPs with two different sizes.²³ One had hydrodynamic diameter of 10.8 ± 2.2 nm and zeta potential of -20 mV. The other had hydrodynamic diameter of 22.9 ± 3.9 nm and zeta potential of -17 mV.

Fabrication of microdisks. Aqueous polyelectrolyte solutions used for fabricating the microdisks included 1 wt% PAH-RITC (pH 5.8), 1 wt% PAH (pH 4.3), 1 wt% PSS (pH 5.8), and 1 wt% PDAC (pH 4.6). All of the above solutions contained 150 mM NaCl. For deposition of polyelectrolytes, each step consisted of soaking the stamp in a polyelectrolyte solution for 12 min, followed by a 1 min wash with water. For deposition of AuNPs, 0.5 mL suspension of AuNPs was added on the stamp and kept for 45 min, followed by a 1 min wash with water. The Raman reporters were loaded into the multilayer film by soaking the stamp carrying the multilayer in ethanol solution of each reporter (25 mL, 50 mM for all reporters) for 24 h at room temperature. After soaking, the stamp was briefly washed with ethanol and dried under a nitrogen stream. To transfer the multilayer from the stamp to a substrate, the stamp was exposed to water vapour generated from a 65 °C water bath for 5 sec and then brought into contact with the substrate. PVA-coated glass slides were used as substrates for characterizing the microdisks with optical microscopy and UV-Vis spectroscopy, and for preparing the microdisk-cell complexes. PVA-coated silicon wafers were used as substrates for characterizing the microdisks with Raman spectroscopy. Freshly cleaved mica plates were used as substrates for characterizing the microdisks with AFM. After being kept in contact for 45 sec, the stamp was peeled off from the substrate. The substrate was then exposed to water vapour generated from a 37 °C water bath for 15 sec to release the particles.

Fabrication of dot-on-pad microparticles. PLGA in acetone (400 µL, 2 wt%) was spin-coated on a stamp at 2,500 RPM for 30 sec. A multilayer was deposited on the stamp as described above. The dot-on-pad microparticles were printed on a PVA-coated slide and released as described above.

Preparation of microdisk-cell complexes. Suspension of K562 cells (500 µL, 10⁶ cells·mL⁻¹) in the medium was added on a microdisk array printed on a PVA-coated glass slide and incubated at 37 °C for 15 min. The microdisk-cell complexes formed spontaneously.

Assessing surface enhanced Raman scattering (SERS) effect. Three sets of stamps (3 stamps in each set) were coated with an AuNPs-polyelectrolyte multilayer. The first and second sets were loaded with 2-naphthalenethiol as described above. Each stamp of the first set was placed in a glass shell vial (50 mL) together with an

open plastic centrifuge tube (2 mL) containing 100 μL BME. The bottle was sealed and kept at the room temperature for 24 h. Each stamp of the second set was placed in a covered but not sealed plastic dish for 24 h at the room temperature. Each stamp of the third set (without 2-naphthalenethiol) was exposed to BME following the same procedure as above. Microdisks were then printed on PVA-coated silicon wafers from all stamps and characterized with Raman spectroscopy as described above.

Characterization. The optical micrographs were obtained using an inverted Nikon Ti epifluorescence microscope equipped with an Andor iXonEM+ 885 EMCCD camera. Atomic force microscopy images were collected using a Bruker Icon system and single-beam silicon cantilever probes (Tap300AI-G, resonance frequency of 320 kHz, normal force constant of 40 $\text{N}\cdot\text{m}^{-1}$) operated at tapping mode in air. A Perkin Elmer 950 spectrophotometer was used to obtain the UV-Vis extinction spectra of the microdisks printed on a PVA-coated glass and the suspension of the home-made AuNPs. A NICOMPTM 380 ZLS system was used to measure hydrodynamic diameters and zeta potential of the AuNPs. A home-built Raman spectrometer equipped with a 785 nm (Toptica DL100 Diode laser), a 600 $\text{gr}\cdot\text{mm}^{-1}$ holographic grating, a 1,024 \times 256 element CCD detector (Wright, Open electrode), and a 50 \times [numerical aperture (N.A.) = 0.8] and 5 \times (N.A. = 0.1) objective lens was used to acquire Raman spectra. All samples were analyzed in the spectral range of 100 - 1,700 cm^{-1} at room temperature. Each spectrum was the result of 3 \times 30 sec exposures that were ensemble averaged. Background of Raman spectra was manually subtracted. A digital camera was used to take photographs of the glass slide on which the microdisks were printed.

Results and discussion

The microdisks were characterized with several physical techniques. Figure 2a shows a glass slide on which an array of microdisks was printed. The 1.4 cm-wide printing area had the same lateral dimensions as the stamp and displayed a uniform bluish color, suggesting that a uniform film-like structure was transferred to the slide from the stamp over the entire printing area. A dark-field optical micrograph (Figure 2b) shows a periodic array of the microdisks with the same lattice and diameter as those of the micropillars of the stamp. It also reveals that the microdisks were bright everywhere within individual microdisks. In contrast, multilayered polyelectrolyte microparticles without AuNPs display a ring-like structure (Inset of Figure 2b). This difference suggests that AuNPs were distributed relatively evenly within the microdisks and responsible for the high brightness of the microdisks through Rayleigh scattering of the incident light. It is interesting to note that microdisks appeared larger in the dark-field micrograph than in the phase-contrast micrograph. Atomic force microscopy (AFM) (Figures 2c and 2d) further shows that the microdisks had a smooth top surface and a uniform thickness. Plotting the thickness of the microdisks against layer number of the AuNPs revealed a linear relationship with a slope of 4.47 nm per layer, indicating that each AuNPs/PDAC bilayer had an average thickness of 4.47 nm (Figure 2e). Note that this average bilayer thickness was smaller than the diameter of the AuNPs, suggesting that there was interpenetration between the adjacent AuNPs/PDAC bilayers. Most importantly, the linear relationship suggests that the amount of the AuNPs in the microdisks can be precisely controlled with the layer number of the AuNPs. The optical properties of the microdisks were characterized with UV-Vis extinction spectroscopy (Figure 2f). Plotting the

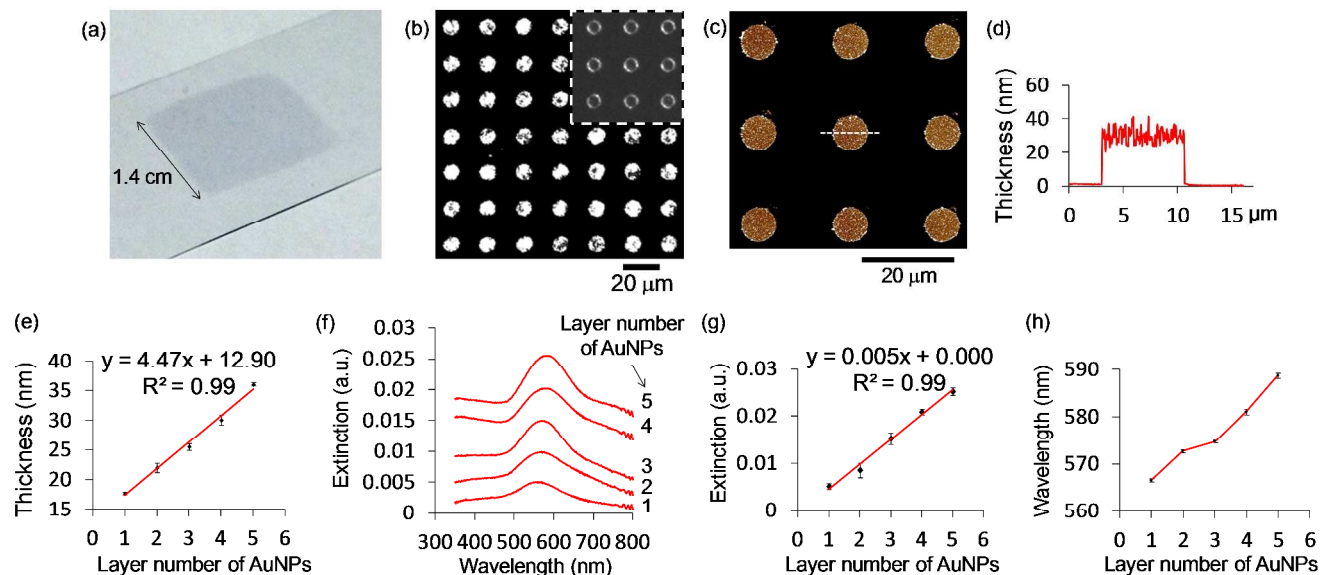


Figure 2. Characterization of printed microdisks. (a) Photograph of a glass slide carrying the printed microdisks. (b) dark-field micrograph of the printed microdisks with 8 μm diameter. Microdisk composition: PAH/(PSS/PDAC)₂/(AuNPs/PDAC)₄/PSS/PDAC. Inset shows a dark-field micrograph of microparticles without AuNPs. Multilayer composition: PAH/(PSS/PDAC)₇. (c) AFM image of microdisks printed on mica. Microdisk composition: PAH/(PSS/PDAC)₂/(AuNPs/PDAC)₃/PSS/PDAC. (d) Line profile of the microdisk crossed by the dashed line in (c). (e) Plot of thickness of the microdisks against layer number of AuNPs. The points represent means and the bars standard deviations (s.d.) of 27 microdisks. The linear fit was included with the corresponding equation. (f) UV-Vis extinction spectra of microdisks with different layer numbers of AuNPs printed on PVA-coated glass slides. Microdisk composition: PAH/(PSS/PDAC)₂/(AuNPs/PDAC)_n/PSS/PDAC, n=1-5. (g) Plot of the UV-Vis extinction at 572 nm against layer number of the AuNPs and the linear fit. The points represent means and the bars s.d. of 5 samples. (h) Plot of UV-Vis extinction peak wavelength against layer number of the AuNPs. The points represent means and the bars s.d. of 3 samples.

extinction at 572 nm against layer number of the AuNPs reveals a linear relationship (Figure 2g), again suggesting that the amount of AuNPs in the microdisks can be controlled with the layer number of the AuNPs. Moreover, the spectra show significant red shifts of the extinction peaks compared to the extinction peak of the AuNPs suspension at 520 nm [Electronic Supplementary Information (ESI) Figure S1] and the shift increases with layer number of the AuNPs (Figure 2h), suggesting that the AuNPs were densely packed in the

microdisks.^{4,24}

The amount of AuNPs in the microdisks can be estimated based on the UV-Vis extinction spectra. First, the microdisk array printed on a glass slide is assumed to be a homogeneous film containing uniformly distributed AuNPs. Second, using Beer-Lambert law, $A = \epsilon c l$, where A is extinction, ϵ extinction coefficient of the AuNPs, c molar density of AuNPs, and l thickness of the film, $c l$ can be

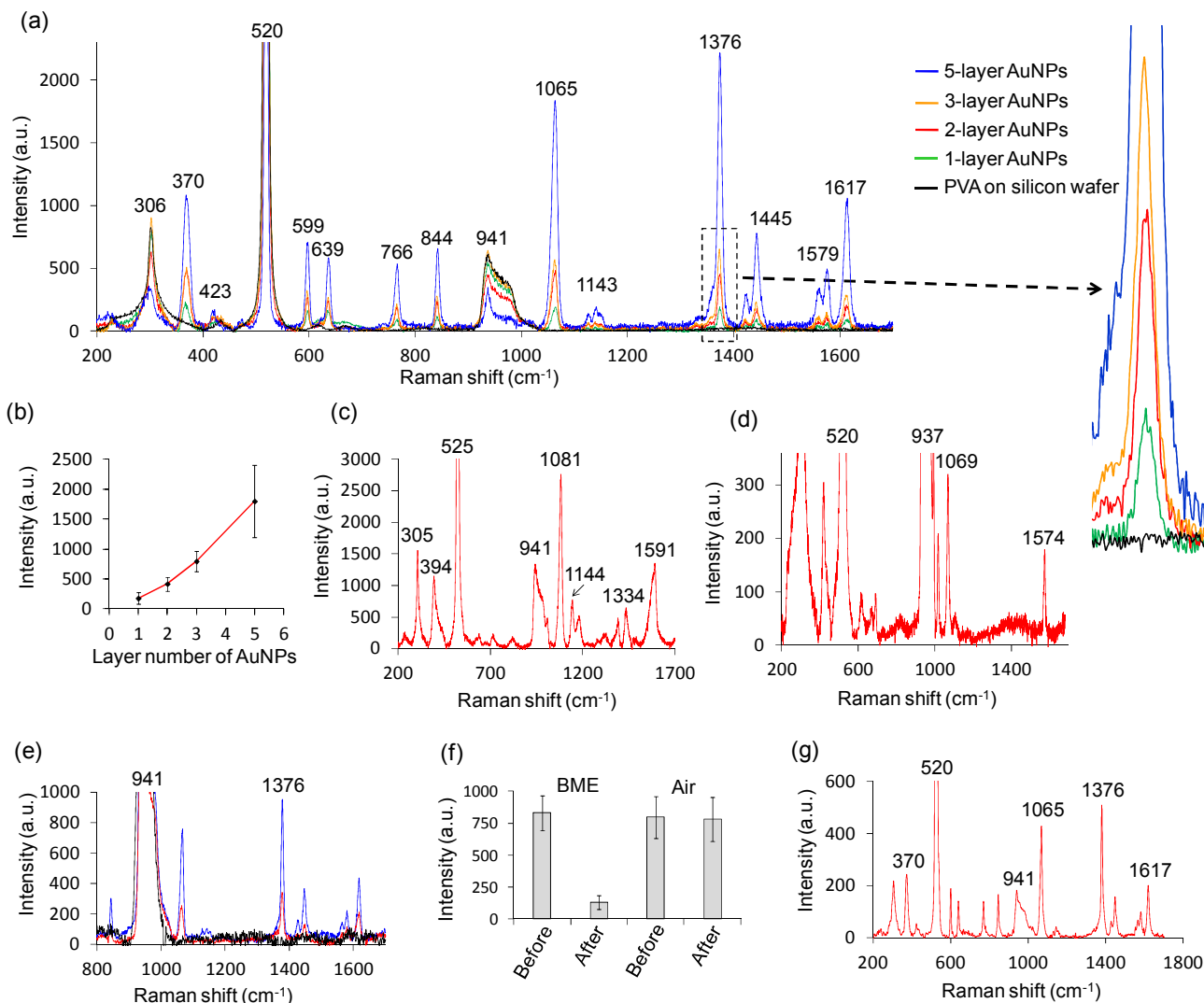


Figure 3. Raman characterization of printed microdisks with PVA-coated silicon wafers as the substrates. The substrates were responsible for the peaks at 306, 520 and 941 cm^{-1} . A $50\times$ objective lens was used to collect all Raman signals except (g). (a) Raman spectra of microdisks containing 1, 2, 3 and 5 layers of AuNPs and loaded with 2-naphthalenethiol. Microdisk composition: PAH/(PSS/PDAC)₂/(AuNPs/PDAC)_n/PSS/PDAC, $n = 1, 2, 3$ and 5. The 1376 cm^{-1} peaks are magnified to reveal details. (b) Plot of Raman signal intensities at 1376 cm^{-1} against layer numbers of the AuNPs. The points represent means and bars s.d. of 12 measurements. Raman spectra of microdisks loaded with (c) 4-aminothiophenol and (d) thiophenol. Microdisk composition: PAH/(PSS/PDAC)₂/(AuNPs/PDAC)₅/PSS/PDAC. (e) Raman spectra of microdisks loaded with 2-naphthalenethiol before (blue line) and after (red line) being exposed to vapour of 2-mercaptoethanol (BME) for 24 h at the room temperature, and blank microdisks (*i.e.* without 2-naphthalenethiol) after being exposed to BME (black line). Microdisk composition: PAH/(PSS/PDAC)₂/(AuNPs/PDAC)₃/PSS/PDAC. (f) Quantitative comparison of Raman signal intensities at 1376 cm^{-1} of the 2-naphthalenethiol-loaded microdisks before and after being exposed to BME vapour and air respectively. Columns represent means and bars s.d. of 9 measurements. (g) Raman spectrum of microdisks containing 2-naphthalenethiol collected with a $5\times$ lens. The AuNPs-polyelectrolyte multilayer on the stamp had been soaked in PBS for 18 h before being printed on a PVA-coated silicon wafer. Microdisk composition: PAH/(PSS/PDAC)₂/(AuNPs/PDAC)₅/PSS/PDAC.

calculated when A and ε are known. For the array of microdisks containing 5 layers of AuNPs, the extinction is 0.0252 at 572 nm. The extinction coefficient ε for the 10 nm-diameter AuNPs is assumed to be $1.0 \times 10^8 \text{ M}^{-1}\text{cm}^{-1}$.²⁵ Thus $c \cdot l$ is calculated as $2.52 \times 10^{-13} \text{ mole}\cdot\text{cm}^{-2}$. Third, considering that the microdisks have a diameter of 8 μm and are arranged in a square lattice with the centre-to-centre distance of 20 μm , $c \cdot l$ of the AuNPs in the microdisks is calculated as $2.01 \times 10^{-12} \text{ mole}\cdot\text{cm}^{-2}$. Finally, since a microdisk has a lateral area of 50.24 μm^2 , the amount of AuNPs packed in each microdisk containing 5 layers of AuNPs is estimated as 6.08×10^5 .

The feasibility of using the microdisks for multiplex Raman labelling was demonstrated with three Raman reporters: 2-naphthalenethiol, 4-aminothiophenol and thiophenol. Each reporter contains a thiol group that can bind to the AuNPs through the thiol-gold bond, thus favouring the surface enhanced Raman scattering (SERS) effect. NIR laser with 785 nm wavelength was used as the excitation light. Raman spectra were first collected from a PVA-coated silicon wafer and then from AuNPs-packed microdisks printed on a PVA-coated wafer. The almost identical spectra shown in ESI Figure S2 indicate that the polyelectrolytes in the microdisks did not produce noticeable Raman signals. Figure 3a shows Raman spectra of microdisks loaded with 2-naphthalenethiol. The characteristic peaks match those in the literature.²⁶ Moreover, the signal intensity increased with the layer number of the AuNPs and therefore the total amount of the AuNPs per microdisk (Figure 3b). In addition to 2-naphthalenethiol, signature Raman spectra of microdisks loaded with 4-aminothiophenol (Figure 3c) and thiophenol (Figure 3d) were also observed,^{27,28} suggesting that the AuNPs-packed microdisks can be used as a universal platform for all thiol-based Raman reporters.

To further assess whether SERS effect contributed to the observed Raman signals, we exposed the 2-naphthalenethiol-loaded microdisks to 2-mercaptoethanol (BME) vapour. Note that 2-naphthalenethiol is a solid at the room temperature and BME is a liquid with a vapour pressure of 1 mmHg according to the vendor. We hypothesized that the vaporized BME molecules could replace some of the 2-naphthalenethiol molecules bound to the AuNPs and the desorbed 2-naphthalenethiol stay trapped in the microdisks. As a result, the average distance between 2-naphthalenethiol and AuNPs would be reduced but the total amount of 2-naphthalenethiol in the microdisks remained unchanged. Because SERS is a highly localized effect,²⁹ we expected to see a significant reduction in SERS signal intensity. The result (Figures 3e and 3f) confirmed this hypothesis. In contrast, 2-naphthalenethiol-loaded microdisks exposed to air did not display a noticeable change in the intensity of the Raman signals. Moreover, the blank microdisk sample did not show any characteristic peaks other than those generated by the substrate, indicating that BME exposure did not contribute to the characteristic peaks of 2-naphthalenethiol. This result suggests that the AuNPs-enabled SERS effect contributed significantly to the observed Raman signals.

The above Raman spectra were collected using a 50 \times objective length operated at a millimetre-scale sample-lens distance. Such a short distance is impractical for non-invasive *in vivo* cell tracking. To alleviate this concern, a 5 \times objective lens operated at a sample-lens distance of ~ 4 cm was used. Moreover, the 2-naphthalenethiol-loaded multilayer on the stamp was soaked in phosphate buffered saline (PBS) for 18 h before printing. Successful acquisition of the characteristic Raman spectra (Figure 3g) suggests that the microdisks can potentially be tracked at a centimetre-scale tissue depth over an extended period of time. AuNPs with diameter of ~ 23 nm were used for this experiment.

The envisioned cell-tracking application also requires attaching the microdisks to human cells. One approach to this end is through releasing the microdisks from the slide first and then allowing the released microdisks to bind to cells *in vitro*. Successful release of the microdisks was demonstrated in Figure 4a. Figure 4b further shows a complex composed of a microdisk and a cell of the K562 human leukemic cell line. The outermost PAH layers of the microdisks were responsible for the microdisk-cell adhesion.³⁰

In addition to producing the AuNPs-packed microdisks, the fabrication method can be easily extended to prepare particulate microdevices with other structures and functionalities. Figure 4c presents an example. Each of the microdevices in this figure consisted of a thermoplastic dot sitting on a pad-like AuNPs-packed microdisk. The microdevices were fabricated by integrating the method introduced in this study with a method that we previously invented.³¹ Since the dot-on-pad structure can offer unique advantages to drug delivery, this type of microdevices can allow synergistic integration of controlled drug delivery and non-invasive *in vivo* tracking of the microdevices.

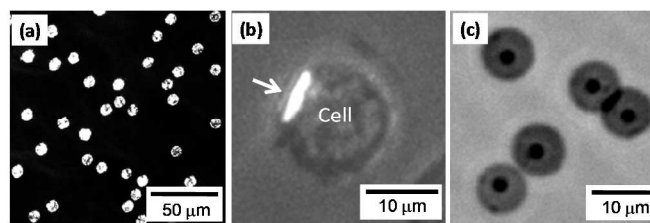


Figure 4. Released microdisks, a microdisk-cell complex and dot-on-pad microdevices. (a) dark-field micrograph of the released microdisks. Microdisk composition: PAH/(PSS/PDAC)₂/(AuNPs/PDAC)₄/PSS/PDAC. (b) Overlaid fluorescence and phase-contrast micrograph of a microdisk-cell complex. The arrowhead points to the microdisk. Microdisk composition: PAH/PSS/(PAH-RITC/PSS)₂/(PDAC/AuNPs)₂/(PAH/PSS)₂/PAH. (c) Phase-contrast micrograph of dot-on-pad microdevices with a thermoplastic dot (black) sitting on a pad-like microdisk (gray). Microdisk composition: (PAH/PSS)₂/(PDAC/AuNPs)₂/(PAH/PSS)₂/PAH. Dot material: poly(D, L-lactide-co-glycolide).

Conclusions

We have developed a novel top-down method for fabricating microdisks containing densely packed AuNPs. The microdisks have a disk-like shape and well-defined structures and dimensions. The amount of the AuNPs per microdisk can be precisely controlled. Multiple thiol-based Raman reporters can be loaded in the microdisks to generate characteristic SERS signals. The signals can be detected at a centimetre-scale sample-lens distance under a NIR excitation. Moreover, the microdisks can be attached to single human cells. The technique promises to be useful for non-invasive tracking of multiple groups of therapeutic cells *in vivo* through multiplexing labelling of the cells.

Acknowledgements

This work was funded by the Florida State University Startup Fund and National Science Foundation award 1300447.

Notes and references

^a Department of Chemical and Biomedical Engineering, FAMU-FSU College of Engineering, Florida State University, 2525 Pottsdamer Street, Tallahassee, Florida, 32310, USA. Fax: 1-850-410-6150; Tel: 1-850-410-6643; E-mail: guan@eng.fsu.edu

^b Integrative NanoScience, Florida State University, Tallahassee, Florida, 32306.

Electronic Supplementary Information (ESI) available: An additional figure. See DOI: 10.1039/b000000x/

- 1 E. C. Dreaden, A. M. Alkilany, X. H. Huang, C. J. Murphy and M. A. El-Sayed, *Chem. Soc. Rev.* 2012, **41**, 2740.
- 2 A. M. Yashchenok, D. Borisova, B. V. Parakhonskiy, A. Masic, B.-E. Pinchasik, H. Möhwald and A. G. Skirtach, *Ann. Phys. (Berlin)* 2012, **524**, 723.
- 3 A. Yashchenok, A. Masic, D. Gorin, B. S. Shim, N. A. Kotov, P. Fratzl, H. Möhwald and A. Skirtach, *Small* 2013, **9**, 351.
- 4 W. F. Dong, G. B. Sukhorukov and H. Mohwald, *Phys. Chem. Chem. Phys.* 2003, **5**, 3003.
- 5 A. G. Skirtach, C. Dejugnat, D. Braun, A. S. Susha, A. L. Rogach, W. J. Parak, H. Mohwald and G. B. Sukhorukov, *Nano Lett.* 2005, **5**, 1371.
- 6 A. G. Skirtach, P. Karageorgiev, B. G. De Geest, N. Pazos-Perez, D. Braun and G. B. Sukhorukov, *Adv. Mater.* 2008, **20**, 506.
- 7 J. B. Song, L. Cheng, A. P. Liu, J. Yin, M. Kuang and H. W. Duan, *J. Am. Chem. Soc.* 2011, **133**, 10760.
- 8 J. B. Song, J. J. Zhou and H. W. Duan, *J. Am. Chem. Soc.* 2012, **134**, 13458.
- 9 J. Lin, S. J. Wang, P. Huang, Z. Wang, S. H. Chen, G. Niu, W. W. Li, J. He, D. X. Cui, G. M. Lu, X. Y. Chen and Z. H. Nie, *Acs Nano* 2013, **7**, 5320.
- 10 J. B. Song, Z. Fang, C. X. Wang, J. J. Zhou, B. Duan, L. Pu and H. W. Duan, *Nanoscale* 2013, **5**, 5816.
- 11 A. Ahmed, C. Bonner and T. A. Desai, *Microdevices* 2001, **3**, 89.
- 12 J. J. Guan, H. Y. He, L. J. Lee and D. J. Hansford, *Small* 2007, **3**, 412.
- 13 D. C. Pregibon, M. Toner and P. S. Doyle, *Science* 2007, **315**, 1393.
- 14 P. Decuzzi, R. Pasqualini, W. Arap and M. Ferrari, *Pharm. Res.* 2009, **26**, 235.
- 15 J. L. Perry, K. P. Herlihy, M. E. Napier and J. M. Desimone, *Acc. Chem. Res.* 2011, **44**, 990.
- 16 A. J. Swiston, C. Cheng, S. H. Um, D. J. Irvine, R. E. Cohen and M. F. Rubner, *Nano Lett.* 2008, **8**, 4446.
- 17 P. P. Zhang and J. J. Guan, *Small* 2011, **7**, 2998.
- 18 E. M. Shapiro, K. Sharer, S. Skrtic and A. P. Koretsky, *Magn. Reson. Med.* 2006, **55**, 242.
- 19 P. D. Acton and R. Zhou, *Q. J. Nucl. Med. Mol. Imaging.* 2005, **49**, 349.
- 20 T. Sugiyama, S. Kuroda, T. Osanai, H. Shichinohe, Y. Kuge, M. Ito, M. Kawabori and Y. Iwasaki, *Neurosurgery* 2011, **68**, 1036.
- 21 U. Mahmood and R. Weissleder, *Mol. Cancer Ther.* 2003, **2**, 489.
- 22 J. Park and P. T. Hammond, *Adv. Mater.* 2004, **16**, 520.
- 23 N. R. Jana, L. Gearheart and C. J. Murphy, *Chem. Mater.* 2001, **13**, 2313.
- 24 M. Brust, D. Bethell, C. J. Kiely and D. J. Schiffrin, *Langmuir* 1998, **14**, 5425.
- 25 X. O. Liu, M. Atwater, J. H. Wang and Q. Huo, *Colloids Surf., B* 2007, **58**, 3.
- 26 P. J. G. Goulet, D. S. dos Santos, R. A. Alvarez-Puebla, O. N. Oliveira and R. F. Aroca, *Langmuir* 2005, **21**, 5576.
- 27 Z. H. Zhu, T. Zhu and Z. F. Liu, *Nanotechnology* 2004, **15**, 357.
- 28 H. Y. Jung, Y. K. Park, S. Park and S. K. Kim, *Anal. Chim. Acta* 2007, **602**, 236.
- 29 K. Kneipp, H. Kneipp, I. Itzkan, R. R. Dasari and M. S. Feld, *Chem. Rev.* 1999, **99**, 2957.
- 30 Z. B. Wang, P. P. Zhang, B. Kirkland, Y. R. Liu and J. J. Guan, *Soft Matter* 2012, **8**, 7630.
- 31 P. P. Zhang, Y. R. Liu, J. F. Xia, Z. B. Wang, B. Kirkland and J. J. Guan, *Adv. Healthc. Mater.* 2013, **2**, 540.